Contribution from the Department of Chemistry, Emory University, Atlanta, Georgia 30322, and Dipartimento di Scienze Chimiche, Università di Trieste, 34127 Trieste, Italy

NMR Studies of Costa-Type Organocobalt Compounds. Structural Characterization of Several 1,5,6-Trimethylbenzimidazole Complexes

Wallace O. Parker, Jr.,† Ennio Zangrando,‡ Nevenka Bresciani-Pahor,‡ Patricia A. Marzilli,† Lucio Randaccio,*,‡ and Luigi G. Marzilli*,†

Received October 14, 1987

^1H and ^{13}C NMR spectral data have been collected and interpreted for several series of Costa-type organocobalt B_{12} model complexes, $[LCo((DO)(DOH)pn)R]ClO_4$ (where L = neutral base, (DO)(DOH)pn = $N^2,N^{2'}$-propanediylbis(2,3-butanedione 2-imine 3-oxime), and R = alkyl ligand). NMR spectra of these complexes in $CDCl_3$ with L = pyridine (py) and R = CH_2CF_3, $CH_2CO_2CH_3$, CH_2Br, CH_3, $CH_2Si(CH_3)_3$, $CH_2C_6H_5$, CH_2CH_3, *neo*-C_5H_{11}, *i*-C_3H_7, and c-C_6H_{11} were determined. The ^1H and ^{13}C NMR spectra of $[H_2OCo((DO)(DOH)pn)R]ClO_4$ (R = CH_2CN, CH_2CF_3, $CH_2CO_2CH_3$, CH_2Br, CH_3, CH_2CH_3, *neo*-C_5H_{11}, *i*-C_3H_7, c-C_6H_{11}) in DMSO-d_6 were collected. ^1H and ^{13}C NMR data for a series containing fewer alkyl derivatives of L = 1,5,6-trimethylbenzimidazole (Me_3Bzm) complexes, dissolved in $CDCl_3$ or DMSO-d_6, were obtained. Relatively large ^1H and ^{13}C NMR signal line widths were found in $[Me_3BzmCo((DO)(DOH)pn)R]ClO_4$ derivatives containing the strongest trans effect alkyl groups (R = *i*-C_3H_7, c-C_6H_{11}). The trends and shift values for the ^1H and ^{13}C NMR data reported here support previous findings that the Co(DO)(DOH)pn moiety is relatively electron poor compared to the $Co(DH)_2$ moiety (DH = monoanion of dimethylglyoxime) and that the magnetic anisotropy of the $Co((DO)(DOH)pn)R^+$ moiety is greater than that of the $Co(DH)_2R$ moiety. Since the Me_3Bzm ligand closely resembles the 5,6-dimethylbenzimidazole ligand in cobalamins, several additional studies were performed. The rate of Me_3Bzm dissociation was found to increase by 10^5 across the series of seven derivatives with different R from CH_2CF_3 to c-C_6H_{11}. The Me_3Bzm ligand in $[Me_3BzmCo((DO)(DOH)pn)R]ClO_4$ dissociated ca. 10 times faster than in the comparable $Me_3BzmCo(DH)_2R$ complexes in CH_2Cl_2 at 25 °C. The three-dimensional structures of $[Me_3BzmCo((DO)(DOH)pn)R]PF_6$, with R = CH_3 (I), R = CH_2CH_3 (II), and R = CH_2CF_3 (III), were determined. Crystallographic details follow. I: $C_{22}H_{34}CoF_6N_6O_2P$, $P2_1/c$, a = 13.238 (2) Å, b = 16.763 (3) Å, c = 13.615 (3) Å, β = 117.20 (2)°, D(calcd) = 1.53 g cm^{-3}, Z = 4, R = 0.046 for 4049 independent reflections. II: $C_{23}H_{36}CoF_6N_6O_2P$, $P2_1/c$, a = 13.233 (2) Å, b = 17.027 (3) Å, c = 14.191 (2) Å, β = 118.32 (1)°, D(calcd) = 1.49 g cm^{-3}; Z = 4, R = 0.047 for 3630 independent reflections. III: $C_{23}H_{33}CoF_9N_6O_2P$, $P2_1/n$, a = 11.765 (3) Å, b = 7.919 (2) Å, c = 31.220 (5) Å, β = 93.42 (2)°, D(calcd) = 1.57 g cm^{-3}, Z = 4, R = 0.045 for 4331 independent reflections. The orientation of the Me_3Bzm ligand in structure III is similar to that observed for py in the two known $[(py)Co((DO)(DOH)pn)R]PF_6$ structures, with the L plane perpendicular to the vertical symmetry plane of the (DO)(DOH)pn moiety. In structures I and II, the angle between the planes is ca. 60°, with the six-membered ring of Me_3Bzm positioned away from the propylene bridge.

Introduction

The physical properties of organocobalt B_{12} model compounds have been reviewed.[1-6] Factors affecting the strength of the Co–C bond in coenzyme B_{12} (5′-deoxyadenosylcobalamin) are of major interest since the biological function of the coenzyme is to provide a 5′-deoxyadenosyl radical by Co–C bond homolysis.[2,4,7]

Corrin ring distortions are thought to weaken the Co–C bond.[2,8] Folding of this ring about the Co–C(10) line, away from the axial benzimidazole ligand in the structures of 5′-deoxyadenosylcobalamin[9] and methylcobalamin[10] has been attributed to the bulkiness of benzimidazole.[9] However, recent 2D NMR studies on coenzyme B_{12} in D_2O indicate that the corrin ring pucker appears to be unaffected by dissociation of the axial dimethylbenzimidazole at low pH.[11]

Small organocobalt complexes have been crucial in providing a foundation for understanding the chemistry of the more complex molecule coenzyme B_{12}.[1-6] Organocobalt complexes containing the $(DH)_2$ equatorial ligand system (where DH = monoanion of dimethylglyoxime) have been characterized most extensively.[6] Research on these B_{12} models (called cobaloximes) has shown that less basic neutral ligands (L) lower the bond dissociation energy (BDE) of the Co–C bond in $LCo(DH)_2CH(CH_3)C_6H_5$.[2,3] Less basic ligands do not stabilize the Co(III) oxidation state as well as more strongly basic ones. Structural data collected on model compounds revealed that the only clear correlation to Co–C BDE's is the Co–L bond length.[12,13] Structural characterization of five-coordinate Co(saloph)R (where saloph = dianion of disalicylidene-*o*-phenylenediamine) complexes established that shorter (stronger) Co–C bonds do exist in complexes with L removed, relative to six-coordinate complexes.[14] Thus, a lengthening of the Co–N (benzimidazole) bond in coenzyme B_{12}, but not removal of L, would favor dissociation of the Co–C bond.

Our recent interest in Costa model systems, $[LCo((DO)(DOH)pn)R]^+$,[15-19] followed reports from Finke's laboratory that a closely related system was an excellent electrochemical mimic of cobalamins.[20,24] Since the initial syntheses of the Costa

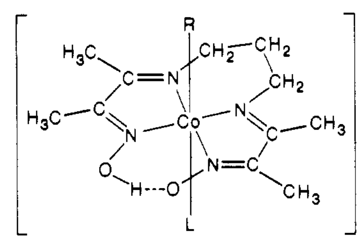

[LCo((DO)(DOH)pn)R]$^+$

† Emory University.
‡ Università di Trieste.

(1) Dolphin, D., Ed. *B*$_{12}$; Wiley: New York, 1982.
(2) Halpern, J. *Science (Washington, D.C.)* **1985**, *227*, 869.
(3) Halpern, J. *Pure Appl. Chem.* **1983**, *55*, 1059.
(4) Finke, R. G.; Schiraldi, D. A.; Mayer, B. J. *Coord. Chem. Rev.* **1984**, *54*, 1. Hay, B. P.; Finke, R. G. *J. Am. Chem. Soc.* **1986**, *108*, 4820.
(5) Toscano, P. J.; Marzilli, L. G. *Prog. Inorg. Chem.* **1984**, *31*, 105.
(6) Bresciani-Pahor, N.; Forcolin, M.; Marzilli, L. G.; Randaccio, L.; Summers, M. F.; Toscano, P. J. *Coord. Chem. Rev.* **1985**, *63*, 1.
(7) Finke, R. G.; Schiraldi, D. A. *J. Am. Chem. Soc.* **1983**, *105*, 7605.
(8) Toraya, T.; Krodel, E.; Mildvan, A. S.; Abeles, R. H. *Biochemistry* **1979**, *18*, 417.
(9) Glusker, J. P. In *B*$_{12}$; Dolphin, D., Ed.; Wiley: New York, 1982; Vol. 1, p 23.
(10) Rossi, M.; Glusker, J. P.; Randaccio, L.; Summers, M. F.; Toscano, P. J.; Marzilli, L. G. *J. Am. Chem. Soc.* **1985**, *107*, 1729.
(11) Bax, A.; Marzilli, L. G.; Summers, M. F. *J. Am. Chem. Soc.* **1987**, *109*, 566.
(12) Summers, M. F.; Marzilli, L. G.; Bresciani-Pahor, N.; Randaccio, L. *J. Am. Chem. Soc.* **1984**, *106*, 4478.
(13) Summers, M. F.; Toscano, P. J.; Bresciani-Pahor, N.; Nardin, G.; Randaccio, L.; Marzilli, L. G. *J. Am. Chem. Soc.* **1983**, *105*, 6259.
(14) Marzilli, L. G.; Summers, M. F.; Bresciani-Pahor, N.; Zangrando, E.; Charland, J.-P.; Randaccio, L. *J. Am. Chem. Soc.* **1985**, *107*, 6880.
(15) Parker, W. O., Jr.; Bresciani-Pahor, N.; Zangrando, E.; Randaccio, L.; Marzilli, L. G. *Inorg. Chem.* **1985**, *24*, 3908.
(16) Parker, W. O., Jr.; Bresciani-Pahor, N.; Zangrando, E.; Randaccio, L.; Marzilli, L. G. *Inorg. Chem.* **1986**, *25*, 1303.
(17) Parker, W. O., Jr.; Zangrando, E.; Bresciani-Pahor, N.; Randaccio, L.; Marzilli, L. G. *Inorg. Chem.* **1986**, *25*, 3489.

compounds,[25-31] relatively little structural, NMR, and L exchange data had been reported. In previous reports, we studied these properties for a large number of alkyl derivatives and concluded that the Costa-type system is a useful model for coenzyme B_{12} on the basis of L-exchange rates, Co–L bond lengths, flexibility of the equatorial ligand, and magnetic anisotropy of the equatorial unit.[15-19] In particular, the dipolar effect of the cobalt anisotropy on the chemical shifts of nearby nuclei is well-known[32] and must be accounted for when NMR shift trends in cobalt complexes are analyzed.[10,33-36] An excellent correlation exists between the ^{13}C NMR γ-C shifts of 4-*tert*-butylpyridine cobaloximes and Co–N bond lengths for a large series of pyridine (py) cobaloximes.[6] Quantitation of the electronic and dipolar effects of cobalt on the ^{13}C shifts of dimethylbenzimidazole could facilitate the interpretation of NMR spectral trends for cobalamins.[34] Hence, this information could be useful in assessing conformational and structural changes that lead to Co–C bond cleavage in coenzyme B_{12} in B_{12} holoenzymes.

In this report we examine structural and L exchange data for Costa models containing 1,5,6-trimethylbenzimidazole (Me_3Bzm), the base most appropriate for comparison with cobalamins. Furthermore, ^1H and ^{13}C NMR data for these complexes and for py adducts are compared with data available for cobaloximes.

Experimental Section

Reagents. Me_3Bzm was prepared by a procedure similar to that given for 1-ethyl-5,6-dimethylbenzimidazole.[37] Solvents were from Fisher. Deuteriated solvents and all other ligands and reagents were obtained from Aldrich. Elemental analyses were performed by Atlantic Microlabs, Atlanta, GA.

Rate Measurements. Ligand substitution reactions were carried out in CH_2Cl_2 and monitored spectrophotometrically with a Perkin-Elmer Lambda 3B instrument equipped with a Model 3600 data station for the slower reactions ($k_{obsd} < 0.05\ s^{-1}$) or a Durrum-Gibson D-110 stopped-flow spectrophotometer for the faster reactions. Both instruments were equipped with thermostated cell compartments (25.0 ± 0.04 °C). Visible spectra of (DO)(DOH)pn complexes in CH_2Cl_2 (0.5–1.5 mM) were recorded before and after addition of an excess (in most cases 100:1) of entering ligand (L′ = trimethyl phosphite), allowing sufficient time for complete reaction (verified by ^1H NMR). Absorbance changes (440–480 nm) over the first $3t_{1/2}$ and the absorbance at $8t_{1/2}$ were used in the calculations. At least three data sets were collected for each complex.

Data Analysis. The rate constants are defined as

$$ML \underset{k_{-1}}{\overset{k_1}{\rightleftharpoons}} M + L$$

$$M + L' \xrightarrow{k_2} ML'$$

where M = Co((DO)(DOH)pn)R and L′ is a suitable entering ligand. The absorbance vs rate data were treated with the standard integrated expression for a first-order process by using a linear least-squares program.

NMR Spectroscopy. ^1H NMR spectra were recorded on a Nicolet NB-360 spectrometer (16K, spectral range (SW) of 9500 Hz). Chemical shifts are relative to internal Me_4Si. The concentration of the complexes in DMSO-d_6 was 0.1 M. Lower concentrations, 5–20 mM, were employed in $CDCl_3$. 1D NOE experiments were performed as previously.[17]

Proton-noise-decoupled ^{13}C NMR spectra were recorded at 22 °C (referenced to internal TMS). The ^{13}C NMR spectra of the H_2O and py derivatives in DMSO-d_6 and $CDCl_3$, respectively, were obtained on a Varian CFT-20 spectrometer (20 MHz). The 8K spectra were collected by using a SW of 4500 Hz, a 25° pulse, no relaxation delay (RD), and ca. 20 000 transients (20 ktrs). The spectra of the Me_3Bzm derivatives ($CDCl_3$) were obtained under the same conditions but with an RD of 0.5 s and 20–60 ktrs. An IBM WP-200SY spectrometer (50.33 MHz) was used to obtain ^{13}C NMR spectra for the Me Bzm derivatives in DMSo-d_6. The 16K spectra were collected using a SW of 15 150 Hz, a 25° pulse, a 0.5 s RD, and 30–50 ktrs. Concentrations of the [LCo((DO)(DOH)pn)R]ClO_4 complexes were 0.1 M in DMSO-d_6 and less in $CDCl_3$ for some complexes, as specified.

Preparation of [LCo((DO)(DOH)pn)R]ClO_4 Complexes. All compounds were stored at 5 °C and handled with minimal exposure to light and to temperatures >35 °C.

[H_2OCo((DO)(DOH)pn)R]ClO_4 (R = CH_2CF_3, $CH_2CO_2CH_3$, CH_2Br, CH_3, $CH_2Si(CH_3)_3$, $CH_2C_6H_5$, CH_2CH_3, *neo*-C_5H_{11}, *i*-C_3H_7, c-C_6H_{11}) complexes were prepared as reported earlier.[15,19]

[Me_3BzmCo((DO)(DOH)pn)R]ClO_4 (R = CH_2CF_3, CH_2Br, CH_3, CH_2CH_3, *neo*-C_5H_{11}, c-C_6H_{11}). A solution of Me_3Bzm (1.2 equiv) in methanol (5–10 mL) was mixed with [H_2OCo((DO)(DOH)pn)R]ClO_4 (0.25 g) in a 25-mL Erlenmeyer flask. The mixture was dissolved with stirring for a few minutes and warmed slightly, and if necessary, acetone (5–10 mL) was added to cause complete dissolution. The red solution was filtered and after addition of H_2O (5–10 mL) left uncovered (23 °C). The crystalline product formed within a few days was collected and washed with diethyl ether. Yields: R = CH_2CF_3, 230 mg (73%); R = CH_2Br, 240 mg (67%); R = CH_3, 220 mg (80%); R = CH_2CH_3, 210 mg (65%); R = *neo*-C_5H_{11}, 300 mg (90%); R = c-C_6H_{11}, 250 mg (81%). Elemental analyses (C, H, N) are given in a supplementary table.[45]

[Me_3BzmCo((DO)(DOH)pn)CH_2CN]ClO_4 was prepared from crude [H_2OCo((DO)(DOH)pn)CH_2CN]ClO_4, which was obtained by treatment of the 1-methylimidazole (1-MeImd) adduct with cation-exchange resin. [1-MeImdCo((DO)(DOH)pn)CH_2CN]ClO_4 was prepared by addition of $ClCH_2CN$ (4.5 mL, 72 mmol) and $NaBH_4$ (1.4 g, 36 mmol in 15 mL of H_2O) to a methanol solution (600 mL) of Co((DO)(DOH)pn)Br_2 (11 g, 24 mmol) and 1-MeImd (3 mL, 36 mmol) as described previously.[15] The solvent was removed by rotoevaporation to produce a dark oil. Acetone (100 mL) was added to the oil, and a white solid was removed by filtration. Aqueous $NaClO_4$ (4 g, 40 mmol in 50 mL of H_2O) was added to the red filtrate, and the solvent was evaporated (to ca. 50 mL) to produce a yellow precipitate. This precipitate was collected and washed with H_2O (100 mL), ethanol (20 mL) and diethyl ether (20 mL). Yield: 7.0 g (56%). This precipitate was dissolved in acetone (400 mL). Dowex 50-X8-100 cation-exchange resin (7 g) was added to the solution, and the mixture was stirred for 2 days. The solution was filtered and acetone was removed from the filtrate by rotoevaporation. The residue left was mostly 1-MeImd adduct (77%) as judged by ^1H NMR spectroscopy in DMSO-d_6. This residue was dissolved in methanol (700 mL), resin (7 g) was added to the solution, and the mixture was stirred for 2 days. The resin was removed by filtration. Aqueous $NaClO_4$ (2 g, 20 mmol in 20 mL of H_2O) was added to the filtrate, and the volume of this solution was reduced (to ca. 30 mL) by rotoevaporation to give a crude precipitate. This precipitate was collected, washed with diethyl ether, and recrystallized from acetone–diethyl ether. Yield: 3.0 g, 50%. The product was the desired complex along with ca. 20% of impurities as judged by ^1H NMR spectroscopy. The crude aqua complex (0.30 g, ca. 60 mmol) was suspended in acetone (80 mL), and Me_3Bzm (0.13 g, 0.81 mmol in 10 mL of acetone) was added with stirring. The mixture was stirred overnight. Any insoluble material was removed by filtration (ca. 0.2 g), and the filtrate was evaporated to dryness by rotoevaporation. The residue that resulted was dissolved in acetone (ca. 10 mL), and diethyl ether was added until the solution became slightly cloudy. Precipitation of the product was induced when

(18) Marzilli, L. G.; Parker, W. O., Jr.; Charland, J.-P.; Summers, M. F.; Randaccio, L.; Bresciani-Pahor, N.; Zangrando, E. In *Frontiers in Bioinorganic Chemistry*; Xavier, A. V., Ed., VCH: Weinheim, FRG, 1986; p 647.
(19) Zangrando, E.; Parker, W. O., Jr.; Bresciani-Pahor, N.; Thomas, L. B.; Marzilli, L. G.; Randaccio, L. *Gazz. Chim. Ital.* **1987**, *117*, 307.
(20) Finke, R. G.; McKenna, W. P.; Schiraldi, D. A.; Smith, B. L.; Pierpoint, C. *J. Am. Chem. Soc.* **1983**, *105*, 7592.
(21) Finke, R. G.; Smith, B. L.; McKenna, W. A.; Christian, P. A. *Inorg. Chem.* **1981**, *20*, 687.
(22) Marzilli, L. G.; Bresciani-Pahor, N.; Randaccio, L.; Zangrando, E.; Myers, S. A.; Finke, R. G. *Inorg. Chim. Acta* **1985**, *107*, 139.
(23) Finke, R. G.; Smith, B. L.; Mayer, B. J.; Molinero, A. A. *Inorg. Chem.* **1983**, *22*, 3677.
(24) Elliot, C. M.; Hershenhart, E.; Finke, R. G.; Smith, B. L. *J. Am. Chem. Soc.* **1981**, *103*, 5558.
(25) Costa, G.; Mestroni, G.; Savorgnani, E. *Inorg. Chim. Acta* **1969**, *3*, 323.
(26) Pellizer, G.; Tauszik, G. R.; Costa, G. *J. Chem. Soc., Dalton Trans.* **1973**, 317.
(27) Bigotto, A.; Costa, G.; Mestroni, G.; Pellizer, G.; Puxeddu, A.; Reisenhofer, E.; Stefani, L.; Tauzher, G. *Inorg. Chem.* **1970**, *4*, 41.
(28) Pellizer, G.; Tauszik, G. R.; Tauzher, G.; Costa, G. *Inorg. Chim. Acta* **1973**, *7*, 60.
(29) Fox, J. P.; Banninger, R.; Proffitt, R. T.; Ingraham, L. L. *Inorg. Chem.* **1972**, *11*, 2379.
(30) Guschl, R. J.; Brown, T. L. *Inorg. Chem.* **1974**, *13*, 959.
(31) Costa, G. *Pure Appl. Chem.* **1972**, *30*, 335.
(32) McConnell, H. M. *J. Chem. Phys.* **1957**, *27*, 226.
(33) Trogler, W. C.; Stewart, R. C.; Epps, L. A.; Marzilli, L. G. *Inorg. Chem.* **1974**, *13*, 1564.
(34) Brown, K. L.; Hakimi, J. M. *J. Am. Chem. Soc.* **1986**, *108*, 496.
(35) Brown, K. L.; Hakimi, J. M.; Nuss, D. M.; Montejano, Y. D.; Jacobsen, D. W. *Inorg. Chem.* **1984**, *23*, 1463.
(36) Stewart, R. C.; Marzilli, L. G. *Inorg. Chem.* **1977**, *16*, 424.
(37) Simonav, A. M.; Pozharskii, A. E.; Marianovskii, V. M. *Ind. J. Chem.* **1967**, *5*, 81.
(38) Summers, M. F.; Marzilli, L. G.; Bax, A. *J. Am. Chem. Soc.* **1986**, *108*, 4285.

Table I. Crystallographic Data for Compounds I–III ($[Me_3BzmCo((DO)(DOH)pn)R]PF_6$) at 18 °C

	I	II	III
R	CH_3	CH_2CH_3	CH_2CF_3
formula	$CoO_2N_6C_{22}$-$H_{34}PF_6$	$CoO_2N_6C_{23}$-$H_{36}PF_6$	$CoF_3O_2N_6C_{23}$-$H_{33}PF_6$
mol wt	618.5	632.5	686.5
a, Å	13.238 (2)	13.233 (2)	11.765 (3)
b, Å	16.763 (3)	17.027 (3)	7.919 (2)
c, Å	13.615 (3)	14.191 (2)	31.220 (5)
β, deg	117.20 (2)	118.32 (1)	93.42 (2)
V, Å^3	2687.2	2814.8	2903.5
D(calcd), g cm^{-3}	1.53	1.49	1.57
D(measd), g cm^{-3}	1.54	1.51	1.57
Z	4	4	4
F(000)	1280	1312	1408
space group	$P2_1/c$	$P2_1/c$	$P2_1/n$
μ, cm^{-1}	7.7	7.3	7.3
% transmissn: min, max	86.7, 99.5	95.4, 99.8	87.6, 99.7
2θ max (Mo Kα), deg	56	56	56
no. of measd reflcns	6949	7272	7614
no. of indep reflcns ($I > 3\sigma(I)$)	4049	3630	4331
R	0.046	0.047	0.045
R_w	0.050	0.050	0.056

the solution was scratched and cooled (0 °C). The precipitate was collected and washed with H_2O (50 mL) and then diethyl ether (10 mL). Yield: 110 mg (28% from aqua complex).

[Me$_3$BzmCo((DO)(DOH)pn)R]PF$_6$ (R = CH$_2$CF$_3$, CH$_3$, CH$_2$CH$_3$, *i*-C$_3$H$_7$) was prepared as for the perchlorate complexes except that a NH_4PF_6 solution (2 equiv in 5 mL of methanol) was added before warming the mixture. In the case of the *i*-C_3H_7 derivative, no acetone was added to effect dissolution and the solution was *not* warmed. Red crystals of the isopropyl derivative formed on evaporation of the solution overnight at 23 °C. Yield: 160 mg (43%). X-ray-quality crystals were obtained within 6 days from the solutions of the other three derivatives left in Erlenmeyer flasks (23 °C). The methyl complex was less soluble than the others and required a larger volume of acetone to effect dissolution of the mixture.

[pyCo((DO)(DOH)pn)R]ClO$_4$. All derivatives except R = c-C_6H_{11} were prepared previously.[15]

[pyCo((DO)(DOH)pn)-c-C$_6$H$_{11}$]ClO$_4$ was prepared from the corresponding aqua complex, which was obtained as previously,[19] except that, after alkylation, 2 N $HClO_4$ was used to neutralize the solution and the steps involving $AgNO_3$ were omitted. [$H_2OCo((DO)(DOH)pn)$-*c*-C_6H_{11}]ClO_4 (0.2 g, 0.39 mmol) was stirred in methanol (5 mL), and py (37 μL, 0.46 mmol) was added. The solution that resulted was treated with H_2O (ca. 3 mL), filtered, and left uncovered (23 °C). A red crystalline powder was collected 3 days later and washed with H_2O and diethyl ether. Yield: 130 mg (60%). Anal. Calcd for $C_{22}H_{35}ClCoN_5O_6$: C, 47.19; H, 6.30; N, 12.50. Found: C, 47.17; H, 6.29; N, 12.50.

X-ray Method—Crystal Data. Crystals of [Me$_3$Bzm(Co(DO)-(DOH)pn)R]PF$_6$, where R = CH_3 (I), CH_2CH_3 (II), and CH_2CF_3 (III), were obtained as detailed above.

Cell dimensions, determined from Weissenberg and precession photographs, were refined on a CAD4 Enraf-Nonius single-crystal diffractometer by the $\omega/2\theta$ scan technique, by using graphite-monochromatized Mo Kα radiation (λ = 0.7107 Å). The crystallographic data are given in Table I. Intensities of three check reflections were measured during the data collection about every 100 reflections. No decay of intensity occurred throughout the data recording. Reflections having intensities $I > 3\sigma(I)$ were corrected for Lorentz and polarization effects, for anomalous dispersion for all the atoms and for absorption *via* ψ scan (maximum/minimum transmission factors in Table I).

Solution and Refinement of the Structures. All of the structures were solved by conventional Patterson and Fourier methods and refined by the full-matrix anisotropic least-squares method. In the final cycles, the contribution of hydrogen atoms at calculated positions (held constant at B = 5.0 Å^2) was included. The final R and R_w values are given in Table I. The final weighting scheme was $w = 1/(\sigma(F)^2 + (pF)^2 + q)$ where p = 0.01 and q = 4.0, for all the structures, chosen so as to maintain $w(|F_o| - |F_c|)^2$ essentially constant over all ranges of $|F_o|$ and $(\sin\theta)/\lambda$.

The PF_6^- anion of III was found to be disordered. The disorder was interpreted as being due to two orientations, each of 0.5 occupancy, differing by a rotation of about 45° around the axial F(4)–P–F(5) direction. All fluorine atom occupancies were fixed on the basis of the respective electron peak density on the Fourier map with atomic scattering factors from ref 39. Final non-hydrogen positional parameters are given in Tables II–IV. Hydrogen atom coordinates, anisotropic thermal parameters and a list of final calculated and observed structure factors are available.[45] All calculations employed the SDP CAD4 programs on a PDP 11/44 computer.

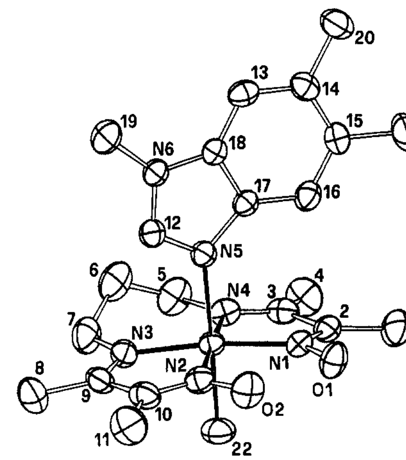

Figure 1. ORTEP drawing (thermal ellipsoid; 50% probability) and labeling scheme for the non-hydrogen atoms of I.

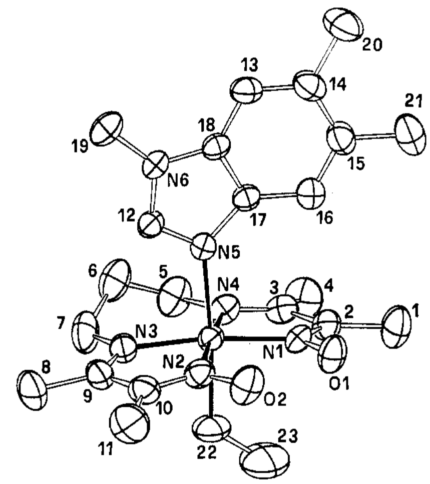

Figure 2. ORTEP drawing (thermal ellipsoid; 50% probability) and labeling scheme for the non-hydrogen atoms of II.

Results

Rate Measurements. The first-order ligand exchange rates (k_1) for [Me$_3$BzmCo((DO)(DOH)pn)R]ClO$_4$ in CH_2Cl_2 (Table V) increase by 10^5 across the series from R = CH_2CF_3 to R = c-C_6H_{11}. On the average, the rates are 10 times larger than those for comparable $(DH)_2$ complexes. A log k_1 vs log k_1 plot for Me$_3$Bzm exchange from the (DO)(DOH)pn and $(DH)_2$ model systems[45] is linear with a slope of 0.94 and a linear correlation coefficient (lcc) = 0.9986 for seven points.

Structural Studies. The ORTEP drawings for non-hydrogen atoms of cations I–III with the atom-numbering scheme are depicted in Figures 1–3. In all of the structures, the (DO)(DOH)pn ligand occupies the four equatorial positions of a distorted octahedron around Co. The chemically equivalent 2,3-butanedione halves of the equatorial ligand are approximately planar, and their planes bend away from Me$_3$Bzm with a rather large dihedral angle, α, of 13.8° in I and even larger values of 16.7° (II) and 16.6° (III) in the derivatives with bulkier alkyls. The displacements of Co out of the mean plane passing through the four N equatorial donors toward N(5) are 0.086 (I), 0.096 (II), and 0.060 Å (III). The central C(6) atom of the propylene bridge is out of the

(39) *International Tables for X-ray Crystallography*; Kynoch: Birmingham, England, 1974; Vol. IV.

Table II. Positional Parameters and Their Estimated Standard Deviations for I

atom	*x*	*y*	*z*	*B*,[a] Å^2
Co	0.15756 (4)	0.20306 (3)	0.12366 (3)	2.272 (8)
O1	0.0019 (2)	0.3226 (2)	0.1142 (2)	3.65 (6)
O2	0.1901 (2)	0.3281 (2)	0.2754 (2)	3.87 (7)
N1	0.0210 (2)	0.2606 (2)	0.0639 (2)	2.58 (6)
N2	0.2393 (2)	0.2685 (2)	0.2467 (2)	2.93 (7)
N3	0.3040 (2)	0.1533 (2)	0.1777 (2)	2.83 (6)
N4	0.0762 (2)	0.1419 (2)	−0.0076 (2)	2.67 (6)
N5	0.1136 (2)	0.1298 (2)	0.2233 (2)	2.48 (6)
N6	0.1421 (2)	0.0401 (2)	0.3541 (2)	2.57 (6)
C1	−0.1681 (4)	0.2812 (3)	−0.0922 (3)	4.4 (1)
C2	−0.0566 (3)	0.2398 (2)	−0.0340 (3)	2.85 (8)
C3	−0.0215 (3)	0.1700 (2)	−0.0750 (3)	2.97 (8)
C4	−0.0943 (4)	0.1397 (3)	−0.1892 (3)	4.4 (1)
C5	0.1252 (4)	0.0723 (3)	−0.0373 (3)	4.1 (1)
C6	0.2207 (4)	0.0344 (3)	0.0627 (3)	4.4 (1)
C7	0.3255 (3)	0.0851 (3)	0.1228 (3)	4.05 (9)
C8	0.5055 (3)	0.1608 (3)	0.3186 (4)	4.9 (1)
C9	0.3837 (3)	0.1864 (2)	0.2629 (3)	3.20 (8)
C10	0.3462 (3)	0.2546 (2)	0.3063 (3)	3.31 (9)
C11	0.4215 (4)	0.3018 (3)	0.4042 (4)	5.1 (1)
C12	0.1887 (3)	0.0873 (2)	0.3056 (3)	2.71 (8)
C13	−0.0627 (3)	0.0190 (2)	0.3142 (3)	2.82 (8)
C14	−0.1718 (3)	0.0444 (2)	0.2455 (3)	2.88 (8)
C15	−0.1907 (3)	0.1041 (2)	0.1648 (3)	2.95 (8)
C16	−0.1015 (3)	0.1363 (2)	0.1523 (3)	2.90 (8)
C17	0.0086 (3)	0.1102 (2)	0.2192 (2)	2.29 (7)
C18	0.0262 (3)	0.0531 (2)	0.3002 (2)	2.31 (7)
C19	0.2033 (3)	−0.0137 (3)	0.4466 (3)	4.0 (1)
C20	−0.2708 (3)	0.0086 (3)	0.2561 (3)	4.0 (1)
C21	−0.3100 (3)	0.1343 (3)	0.0922 (4)	4.5 (1)
C22	0.2047 (3)	0.2758 (3)	0.0345 (3)	3.57 (9)
P	0.54407 (9)	0.38443 (7)	0.15958 (9)	4.00 (3)
F1	0.4931 (3)	0.3018 (2)	0.1649 (3)	10.2 (1)
F2	0.4542 (3)	0.3905 (2)	0.0336 (2)	7.7 (1)
F3	0.6008 (3)	0.4658 (2)	0.1562 (3)	9.7 (1)
F4	0.6339 (3)	0.3764 (2)	0.2856 (3)	7.7 (1)
F5	0.4619 (3)	0.4280 (3)	0.1933 (3)	10.7 (1)
F6	0.6284 (2)	0.3411 (2)	0.1241 (3)	8.4 (1)

[a] Values for anisotropically refined atoms are given in the form of the isotropic equivalent thermal parameter defined as $(4/3)[a^2B(1,1) + b^2B(2,2) + c^2B(3,3) + ab(\cos\gamma)B(1,2) + ac(\cos\beta)B(1,3) + bc\cos\alpha)B(2,3)]$.

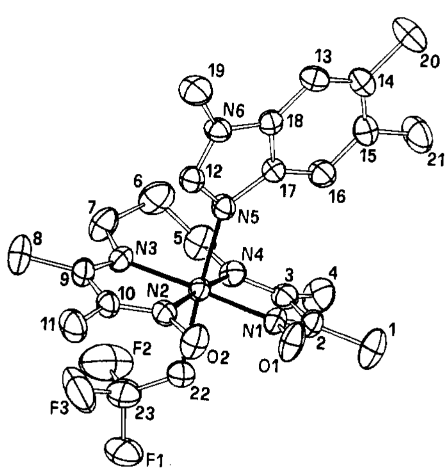

Figure 3. ORTEP drawing (thermal ellipsoid; 50% probability) and labeling scheme for the non-hydrogen atoms of III.

equatorial plane on the Me_3Bzm side in all three structures.

Planar L ligands can have two ideal orientations with respect to the O···H···O group. The staggered orientation, A in Figure 4a, is most commonly found in (DO)(DOH)pn compounds. The eclipsed orientation, B in Figure 4a, is most commonly found in $(DH)_2$ systems. The Me_3Bzm ligand is almost planar in all structures, and the orientation of its plane, with respect to the (DO)(DOH)pn moiety, in III is significantly different from that in I and II (Figure 4b). In I and II, the plane of the Me_3Bzm

Table III. Positional Parameters and Their Estimated Standard Deviations for II

atom	*x*	*y*	*z*	*B*,[a] Å^2
Co	0.16066 (4)	0.19254 (3)	0.13750 (4)	2.564 (9)
O1	−0.0010 (2)	0.3050 (2)	0.1284 (2)	3.92 (7)
O2	0.1870 (3)	0.3116 (2)	0.2883 (2)	4.47 (8)
N1	0.0215 (3)	0.2481 (2)	0.0778 (2)	2.87 (7)
N2	0.2387 (3)	0.2540 (2)	0.2616 (2)	3.35 (8)
N3	0.3100 (3)	0.1457 (2)	0.1930 (2)	3.22 (7)
N4	0.0836 (3)	0.1375 (2)	0.0044 (2)	3.11 (8)
N5	0.1132 (2)	0.1127 (2)	0.2229 (2)	2.67 (7)
N6	0.1407 (2)	0.0187 (2)	0.3424 (2)	2.73 (7)
C1	−0.1667 (4)	0.2727 (3)	−0.0786 (4)	4.9 (1)
C2	−0.0547 (3)	0.2301 (3)	−0.0197 (3)	3.13 (9)
C3	−0.0154 (3)	0.1660 (3)	−0.0621 (3)	3.16 (9)
C4	−0.0844 (4)	0.1412 (3)	−0.1758 (4)	4.8 (1)
C5	0.1369 (4)	0.0741 (3)	−0.0277 (3)	4.5 (1)
C6	0.2324 (4)	0.0338 (3)	0.0683 (4)	4.8 (1)
C7	0.3366 (3)	0.0833 (3)	0.1368 (3)	4.7 (1)
C8	0.5129 (4)	0.1545 (4)	0.3354 (4)	5.6 (1)
C9	0.3882 (3)	0.1778 (3)	0.2794 (3)	3.8 (1)
C10	0.3475 (3)	0.2416 (3)	0.3207 (3)	3.8 (1)
C11	0.4217 (4)	0.2906 (3)	0.4166 (4)	5.9 (2)
C12	0.1884 (3)	0.0657 (2)	0.2976 (3)	2.76 (8)
C13	−0.0635 (3)	0.0059 (3)	0.3091 (3)	3.39 (9)
C14	−0.1722 (3)	0.0361 (3)	0.2483 (3)	3.8 (1)
C15	−0.1905 (3)	0.0973 (3)	0.1742 (3)	3.8 (1)
C16	−0.1017 (3)	0.1268 (3)	0.1597 (3)	3.5 (1)
C17	0.0083 (3)	0.0953 (2)	0.2201 (3)	2.67 (8)
C18	0.0250 (3)	0.0367 (2)	0.2943 (3)	2.70 (8)
C19	0.2022 (4)	−0.0359 (3)	0.4302 (3)	4.3 (1)
C20	−0.2708 (4)	0.0030 (4)	0.2616 (4)	5.7 (1)
C21	−0.3096 (4)	0.1317 (4)	0.1079 (4)	6.0 (2)
C22	0.2198 (4)	0.2675 (3)	0.0625 (4)	4.9 (1)
C23	0.1544 (6)	0.3246 (4)	−0.0095 (5)	10.1 (2)
P	0.5426 (1)	0.38135 (9)	0.1649 (1)	5.08 (3)
F1	0.5042 (3)	0.2973 (2)	0.1785 (3)	10.2 (1)
F2	0.4463 (3)	0.3811 (3)	0.0451 (3)	9.4 (1)
F3	0.5876 (3)	0.4635 (2)	0.1515 (3)	10.6 (1)
F4	0.6401 (3)	0.3807 (3)	0.2847 (3)	10.3 (1)
F5	0.4609 (3)	0.4212 (3)	0.1987 (3)	11.4 (1)
F6	0.6277 (3)	0.3410 (2)	0.1302 (3)	9.2 (1)

[a] See footnote *a* in Table II.

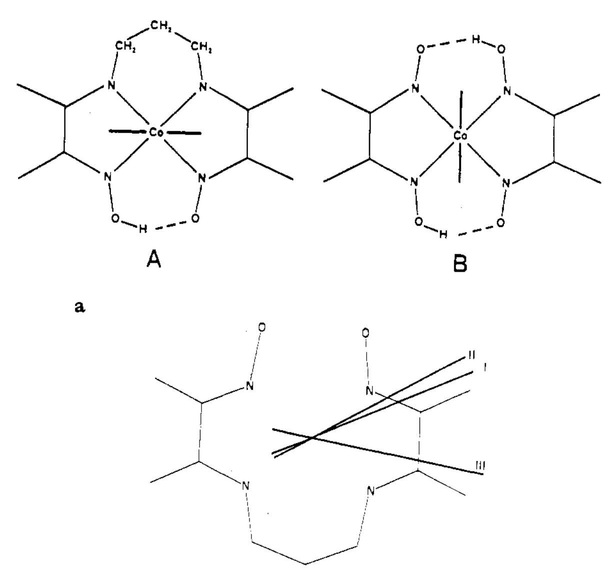

Figure 4. (a) Staggered (A) and eclipsed (B) orientations of planar L, illustrated with the (DO)(DOH)pn and $(DH)_2$ systems, respectively. (b) Approximate orientation of the Me_3Bzm plane, from N6 to C21 (or N1 to B11 by conventional designation), with respect to the (DO)(DOH)pn moiety in structures I–III.

ligand crosses the ON═CMe bonds, whereas in III it bisects the MeC—CMe bonds. We define a torsion angle, ϕ, C(12)–N(5)–Co–N* where N* is the midpoint between N(1) and N(2). The choice of N* is such that the eclipsed conformation (B in

Table IV. Positional Parameters and Their Estimated Standard Deviations for III

atom	x	y	z	B,[a] Å^2
Co	0.31679 (4)	0.11882 (6)	0.10840 (2)	2.079 (8)
F1	0.3122 (3)	−0.2228 (4)	0.00247 (9)	5.27 (7)
F2	0.3444 (4)	0.0418 (5)	0.0006 (1)	9.4 (1)
F3	0.1804 (3)	−0.0485 (5)	0.0146 (1)	8.97 (9)
O1	0.3247 (3)	−0.1242 (4)	0.1748 (1)	4.15 (6)
O2	0.1352 (2)	−0.0686 (4)	0.1406 (1)	3.74 (6)
N1	0.3849 (3)	−0.0316 (4)	0.1488 (1)	2.69 (6)
N2	0.1648 (3)	0.0513 (4)	0.1134 (1)	2.51 (6)
N3	0.2452 (3)	0.2661 (4)	0.0665 (1)	2.60 (6)
N4	0.4721 (3)	0.1684 (4)	0.0994 (1)	2.69 (6)
N5	0.3007 (3)	0.3019 (4)	0.1545 (1)	2.50 (6)
N6	0.2079 (3)	0.4826 (4)	0.1946 (1)	2.72 (6)
C1	0.5589 (4)	−0.1634 (7)	0.1797 (2)	5.0 (1)
C2	0.4953 (3)	−0.0457 (5)	0.1499 (1)	2.95 (8)
C3	0.5443 (3)	0.0708 (5)	0.1199 (1)	2.80 (8)
C4	0.6706 (4)	0.0729 (7)	0.1153 (2)	4.2 (1)
C5	0.5052 (4)	0.2981 (6)	0.0694 (2)	3.9 (1)
C6	0.4203 (4)	0.4397 (6)	0.0651 (2)	4.6 (1)
C7	0.3062 (4)	0.3960 (6)	0.0432 (2)	4.0 (1)
C8	0.0638 (4)	0.3400 (7)	0.0278 (2)	4.5 (1)
C9	0.1370 (3)	0.2440 (5)	0.0598 (1)	2.96 (8)
C10	0.0875 (3)	0.1158 (5)	0.0868 (1)	2.67 (7)
C11	−0.0329 (4)	0.0627 (7)	0.0838 (2)	3.9 (1)
C12	0.2037 (3)	0.3805 (5)	0.1605 (1)	2.74 (7)
C13	0.3689 (3)	0.5541 (5)	0.2488 (1)	2.96 (8)
C14	0.4825 (3)	0.5247 (6)	0.2586 (1)	3.01 (8)
C15	0.5432 (3)	0.4128 (6)	0.2331 (1)	3.13 (9)
C16	0.4907 (3)	0.3329 (6)	0.1982 (1)	3.15 (8)
C17	0.3758 (3)	0.3617 (5)	0.1877 (1)	2.41 (7)
C18	0.3172 (3)	0.4739 (5)	0.2130 (1)	2.37 (7)
C19	0.1148 (4)	0.5831 (6)	0.2102 (2)	4.0 (1)
C20	0.5428 (4)	0.6133 (7)	0.2962 (2)	4.5 (1)
C21	0.6686 (4)	0.3809 (8)	0.2439 (2)	5.0 (1)
C22	0.3283 (4)	−0.0792 (5)	0.0678 (1)	3.29 (9)
C23	0.2899 (5)	−0.0765 (6)	0.0233 (2)	4.7 (1)
P	0.6747 (1)	0.0663 (2)	0.39043 (5)	4.35 (3)
F4	0.6524 (3)	0.2039 (5)	0.3548 (1	7.64 (9)
F5	0.6978 (3)	−0.0704 (4)	0.4271 (1)	6.49 (8)
F6	0.6674 (9)	0.201 (1)	0.4259 (2)	10.8 (3)
F6*	0.7587 (9)	0.187 (1)	0.4140 (3)	13.0 (3)
F7	0.8044 (6)	0.096 (1)	0.3899 (3)	11.0 (2)
F7*	0.7717 (7)	−0.010 (1)	0.3663 (3)	9.6 (2)
F8	0.688 (1)	−0.069 (1)	0.3548 (3)	13.8 (4)
F8*	0.5911 (7)	−0.058 (1)	0.3669 (3)	9.4 (2)
F9	0.5476 (6)	0.030 (1)	0.3887 (3)	11.1 (3)
F9*	0.5735 (8)	0.136 (1)	0.4159 (3)	11.8 (2)

[a] See footnote *a* in Table II.

Table V. First-Order Rate Constants (s^{-1}) for Me_3Bzm Exchange of $Me_3BzmCo(chel)R$ in CH_2Cl_2 (25 °C)

	rate const	
R	chel = (DO)(DOH)pn	chel = $(DH)_2$[c]
CH_2CF_3	$(2.36 \pm 0.07) \times 10^{-4}$	$(1.30 \pm 0.04) \times 10^{-5}$
CH_2Br	$(2.66 \pm 0.05) \times 10^{-3}$	$(1.23 \pm 0.03) \times 10^{-4}$
CH_3	$(4.34 \pm 0.06) \times 10^{-2}$[a]	$(4.19 \pm 0.04) \times 10^{-3}$
CH_2CH_3	$(8.2 \pm 0.1) \times 10^{-1}$	$(1.13 \pm 0.05) \times 10^{-1}$
neo-C_5H_{11}	$(1.01 \pm 0.05) \times 10$	1.23 ± 0.06
i-C_3H_7	$(4.4 \pm 0.2) \times 10$[b]	3.8 ± 0.1
c-C_6H_{11}	$(5.3 \pm 0.3) \times 10$	6.1 ± 0.2

[a] $k_1 = (4.0 \pm 0.1) \times 10^{-2}$ s^{-1} for the PF_6^- salt. [b] Rate constant given is for PF_6^- salt. [c] Reference 42.

Figure 4a) corresponds to $\phi = 0°$. The absolute values of ϕ are 115 (I), 119 (II), and 80° (III).

As already observed in CH_2X cobaloxime derivatives,[6] the alkyl groups in II and III are oriented with respect to the equatorial plane in such a way that the C–X bond is approximately eclipsed with respect to a Co–N(eq) bond. However, in II N(eq) is the oxime N(2) atom, while in III it is the imine N(3) atom.

Selected bond lengths and angles are given in Tables VI and VII. Comparison of the geometry of the axial fragment shows that the Co–C bond length in I is shorter than those in the bulkier alkyl complexes II and III. As expected, the Co–N(axial) distance in I and II is longer than that found in III, which has the poor-electron-donor CH_2CF_3 group. The deviation of the N(5)–Co–C(22) angle from 180° follows the order: I (177.4 (1)°) < II (175.5 (2)°) < III (173.9 (1)°). Although the Co–N(5) bond lengths are different, the values of bond angles around N(5) are very similar in the three structures and are within the range 122.4 (3)–123.1 (2)° for the Co–N(5)–C(12) angle, 132.3 (3)–133.1 (2)° for the Co–N(5)–C(17) angle, and 104.3 (3)–104.8 (3)° for the C(12)–N(5)–C(17) angle. Bond lengths and angles in Me_3Bzm are very similar.

Table VI. Selected Bond Lengths (Å) with Estimated Standard Deviations for I–III

	I	II	III
Co–N1	1.876 (3)	1.876 (3)	1.880 (3)
Co–N2	1.877 (3)	1.881 (3)	1.882 (3)
Co–N3	1.921 (3)	1.919 (3)	1.911 (3)
Co–N4	1.909 (3)	1.913 (3)	1.906 (3)
Co–N5	2.100 (3)	2.105 (3)	2.060 (3)
Co–C22	2.011 (3)	2.041 (4)	2.026 (4)
O1–O2	2.456 (4)	2.448 (4)	2.454 (3)

Table VII. Selected Bond Angles (deg) for I–III

	I	II	III
N1–Co–N2	97.7 (1)	97.3 (1)	97.7 (1)
N1–Co–N3	173.5 (1)	173.3 (1)	178.3 (1)
N1–Co–N4	81.4 (1)	81.5 (1)	81.7 (1)
N1–Co–N5	94.8 (1)	95.1 (1)	91.7 (1)
N1–Co–C22	86.0 (1)	89.2 (2)	83.6 (1)
N2–Co–N3	81.0 (1)	81.1 (2)	81.3 (1)
N2–Co–N4	176.0 (1)	174.9 (1)	174.1 (1)
N2–Co–N5	89.0 (1)	90.1 (1)	90.8 (1)
N2–Co–C22	88.4 (1)	88.0 (2)	86.0 (1)
N3–Co–N4	99.4 (1)	99.5 (2)	99.2 (1)
N3–Co–N5	91.6 (1)	91.5 (1)	89.7 (1)
N3–Co–C22	87.6 (1)	84.2 (2)	95.0 (1)
N4–Co–N5	95.0 (1)	95.0 (1)	95.0 (1)
N4–Co–C22	87.6 (1)	87.0 (2)	88.1 (1)
N5–Co–C22	177.4 (1)	175.5 (2)	173.9 (1)
Co–N5–C12	122.8 (2)	122.4 (3)	123.1 (2)
Co–N5–C17	132.3 (2)	133.1 (2)	132.4 (2)
C12–N5–C17	104.8 (3)	104.6 (4)	104.3 (3)
Co–C22–C23		124.5 (4)	124.4 (3)
C5–C6–C7	115.7 (4)	116.3 (4)	115.9 (4)

NMR Studies. ^1H and ^{13}C NMR spectra were recorded for py and aqua adducts in $CDCl_3$ and DMSO-d_6, respectively, and for the Me_3Bzm adducts in both solvents. Data for cobaloximes are included in most tables for comparison. The [LCo((DO)(DOH)pn)R]X complexes are arranged by the trans effect of the alkyl groups established by py[15] and now Me_3Bzm exchange rates. Also, the electronic parameter (EP) of the R group,[40] developed from ^{13}C NMR data for $Co(DH)_2$ compounds, is employed here to rank the R groups by relative electron-donating ability.

^{1}H NMR Studies. The six equatorial ligand resonances of [pyCo((DO)(DOH)pn)R]ClO_4 complexes in $CDCl_3$ depend very little on R (Table VIII). Thus, the assignments for the CH_3 derivative from 1D NOE studies[17] should apply. All equatorial ^1H NMR signals (except that for O–H···O) of the $CH_2C_6H_5$ derivative are the furthest upfield in the series, due to dipolar shielding by the phenyl ring of $CH_2C_6H_5$. The upfield multiplets from N–CH_2–C–CH_2–N and N–C–CH_2–C–N are more affected by $CH_2C_6H_5$ than are the downfield multiplets, supporting the assignments of the upfield multiplets to the propylene protons closest to $CH_2C_6H_5$.

All ^1H NMR signals of [pyCo((DO)(DOH)pn)-*i*-C_3H_7]ClO_4 in $CDCl_3$ were unusually broad. Addition of py sharpened all signals, except those of free and coordinated py. The c-C_6H_{11} derivative was not very soluble in $CDCl_3$. In CD_2Cl_2, only the py and C=N=C–CH_3 signals were broad. When the sample was cooled to −30 °C, the signals sharpened with a slight shifting

(40) Zangrando, E.; Bresciani-Pahor, N.; Randaccio, L.; Charland, J. P.; Marzilli, L. G. *Organometallics* **1986**, *5*, 1938.

Inorganic Chemistry, Vol. 27, No. 12, 1988

Table VIII. ^1H NMR Chemical Shifts (ppm) of py, $[pyCo((DO)(DOH)pn)R]ClO_4$, and $pyCo(DH)_2R$ Complexes in $CDCl_3$

	chem shift									
compd	α	β	γ	O—H···O	N—CH₂—C—CH₂—N[a]		C—N=C—CH₃	O—N=C—CH₃	N—C—CH₂—C—N[a]	
py	8.61	7.29	7.68							
R = CH_2CF_3										
(DO)(DOH)pn	7.90	7.56	7.80	18.48	4.19	3.77	2.53	2.37	2.22	1.97
R = $CH_2CO_2CH_3$										
(DO)(DOH)pn	7.87	7.55	7.78	18.46	4.14	3.71	2.55	2.41	2.30	1.85
$(DH)_2$	8.51	7.31	7.73	18.18				2.20		
R = CH_2Br										
(DO)(DOH)pn	8.09	7.57	7.82	18.50	4.13	3.86	2.50	2.35	2.20	
$(DH)_2$	8.55	7.33	7.75	*e*				2.18		
R = CH_3										
(DO)(DOH)pn	8.03	7.56	7.80	18.80	4.07	3.79	2.45	2.30	2.08	
$(DH)_2$	8.61	7.33	7.73	18.32				2.13		
R = $CH_2Si(CH_3)_3$										
(DO)(DOH)pn	7.89	7.53	7.76	18.92	4.12	3.70	2.47	2.33	2.26	1.95
R = $CH_2C_6H_5$										
(DO)(DOH)pn	7.82	7.49	7.74	18.69	4.05	3.60	2.29	2.20	*b*	1.75
R = CH_2CH_3										
(DO)(DOH)pn	7.99	7.54	7.78	18.74	4.05	3.68	2.45	2.32	2.11	2.00
$(DH)_2$	8.60	7.31	7.74					2.10		
R = *neo*-C_5H_{11}										
(DO)(DOH)pn	7.84	7.52	7.76	19.01	4.13	3.66	2.48	2.34	2.25	1.84
R = *i*-C_3H_7[c]										
(DO)(DOH)pn	7.96	7.52	7.76	18.58	4.12	3.70	2.45	2.33	2.14	1.99
$(DH)_2$	8.60	7.28	7.70							
R = c-C_6H_{11}[c,d]										
(DO)(DOH)pn	7.99	7.51	7.76	18.58	4.11	3.71	2.43	2.32	ca. 2.13	
$(DH)_2$	8.56	7.26	7.67	*e*				2.12		

[a] Gives rise to two multiplets; values given are the centers of the multiplets. The downfield multiplets arise from the propylene protons nearest L. [b] Obscured by the O—N=C—CH₃ signal. [c] Signals have increased line widths. [d] PF_6^- salt. [e] Data not collected.

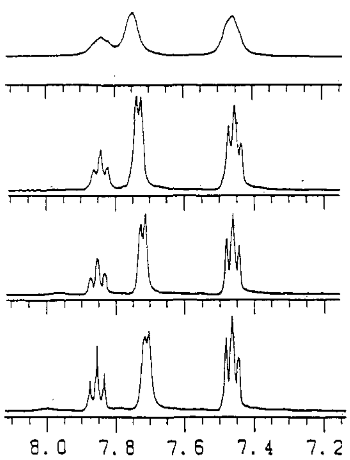

Figure 5. Partial ^1H NMR spectra of $[pyCo((DO)(DOH)pn)$-c-$C_6H_{11}]PF_6$ in CD_2Cl_2 at the following temperatures, listed from top to bottom: 17, 0, −20, −30 °C.

of the py signals (Figure 5). The downfield multiplet from N–CH₂–C–CH₂–N was assigned to protons on the L side, since irradiation of this multiplet enhanced the α-H signals.

Relative to free py, the Co((DO)(DOH)pn) moiety shields the closest H (α) of coordinated py, while H atoms further away (β, γ) are deshielded. These shifts in the $CH_2CO_2CH_3$, CH_3, CH_2CH_3, and *i*-C_3H_7 derivatives of (DO)(DOH)pn complexes are consistently different from those of $(DH)_2$ as follows (with negative values upfield): α, −0.60 ppm; β, +0.23 ppm; γ, +0.05 ppm.

The assignments of the ^1H NMR signals of Me_3Bzm (see **1**),

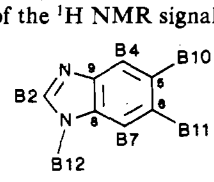

1

free and complexed as $[Me_3BzmCo((DO)(DOH)pn)CH_3]ClO_4$ in $CDCl_3$ (Table IX), are known from 1D NOE experiments.[17] The H2 signal, sharpest of the three methine signals, is the furthest downfield for both compounds. The signals were assigned by assuming that H2 and H7 were the furthest downfield and upfield methine signals, respectively. 1D NOE studies have revealed that the equatorial methyl groups (C—N=C—CH₃) have ^1H signals downfield from the O—N=C—CH₃ signals in this type of complex.[17] Comparison of spectra for R = CH_2CF_3, CH_2Br, CH_3, and CH_2CH_3 in $CDCl_3$ (Table IX) revealed that in each case three signals, H2, B12H₃, and the downfield multiplet of N–CH₂–C–CH₂–N, are downfield for the ClO_4^- relative to the PF_6^- salts (Table IX). The B12H₃ and N–CH₂–C–CH₂–N signals shift by ≤0.10 ppm, and the H2 signals shifts by ca. 0.25 ppm. Line broadening was observed for *i*-C_3H_7 and c-C_6H_{11} derivatives as discussed above for the py analogues. There are no discernible correlations between the ^1H NMR shifts, which are similar across the series, and the donor ability of R (Table IX). H2 and H4 shift the most, 0.3 and 0.2 ppm upfield, respectively, from the CH_2CN to the neo-C_5H_{11} complex. Compared to free Me_3Bzm, most of the signals shift very slightly upfield, with H4 (0.35 ppm average) influenced most.

The H2 and H4 signals in the (DO)(DOH)pn derivatives are substantially upfield from those in the $(DH)_2$ complexes (ca. 0.2 and 0.7 ppm, respectively) (Table IX). Note that for $(DH)_2$ derivatives in $CDCl_3$ the H4 signal is found downfield from the H2 signal,[17] contrary to the situation in the (DO)(DOH)pn derivatives. The B12H₃, O—H···O, and O—N=C—CH₃ ^1H signals are all downfield in the (DO)(DOH)pn compared to those in the $(DN)_2$ derivatives.

From ^1H NMR spectra of the $[Me_3BzmCo((DO)(DOH)pn)R]ClO_4$ complexes dissolved in DMSO-d_6 (Table X), it is apparent that both coordinated and free Me_3Bzm exist in all solutions. The formation constant for $[Me_3BzmCo((DO)(DOH)pn)CH_3]ClO_4$ in DMSO-d_6 was found to be 75 M^{-1}, determined with complex concentrations of 10 and 50 mM by integration of the ^1H NMR signals from O–H···O and Co–CH₃ (for the py adduct K_f = 56 M^{-1}).

Assignments for Me_3Bzm in DMSO-d_6 (Table X) were confirmed by 1D NOE studies performed as previously.[17] Partial saturation of the B12H₃ signal enhanced the H2 and H7 signals (assigning H4). Partial saturation of the downfield signal for either B10H₃ or B11H₃ enhanced H7, assigning it to B11H₃.

Table IX. Chemical Shifts (ppm) of ^1H NMR Signals of Me_3Bzm, $[Me_3BzmCo((DO)(DOH)pn)R]X$, and $Me_3BzmCo(DH)_2R$[a] Complexes in $CDCl_3$

		chem shift										
compd	X	H2	H4	H7	$B11H_3$	$B10H_3$	$B12H_3$	O—H···O	N—CH₂—C—CH₂—N[b]		C—N=C—CH_3	O—N=C—CH_3
Me_3Bzm		7.74	7.56	7.15	2.41	2.39	3.79					
R = CH_2CN												
(DO)(DOH)pn	ClO_4	7.76	7.35	7.15	2.36	2.35	3.95	18.99	4.26	4.00	2.56	2.39
$(DH)_2$		7.92	7.95	7.08	2.37	2.35	3.76	18.49				2.22
R = CH_2CF_3												
(DO)(DOH)pn	PF_6	7.39	7.15	7.13	2.34	2.33	3.85	18.89	4.15	3.80	2.47	2.35
(DO)(DOH)pn	ClO_4	7.73	7.16	7.14	2.34	2.32	3.95	18.88	4.28	3.80	2.51	2.36
$(DH)_2$		7.96	7.98	7.07	2.37	2.35	3.75	18.48				2.14
R = $CH_2CO_2CH_3$												
(DO)(DOH)pn	ClO_4	7.61	7.08	7.15	2.33	2.31	3.91	18.85	4.18	3.75	2.53	2.41
$(DH)_2$		7.93	7.99	7.07	2.38	2.35	3.75	18.44				2.19
R = CH_2Br												
(DO)(DOH)pn	PF_6	7.53	7.29	7.16	2.31	2.29	4.00	19.03	4.02	3.81	2.40	2.28
(DO)(DOH)pn	ClO_4	7.77	7.30	7.15	2.35	2.33	3.95	18.90	4.15	2.85	2.47	2.33
$(DH)_2$		7.94	7.95	7.09	2.37	2.35	3.76	18.43				2.15
R = CH_3												
(DO)(DOH)pn	PF_6	7.46	7.22	7.14	2.35	2.32	3.85	19.24	4.04	3.76	2.37	2.29
(DO)(DOH)pn	ClO_4	7.68	7.22	7.15	2.35	2.32	3.92	19.23	4.11	3.79	2.41	2.29
$(DH)_2$		7.95	7.98	7.08	2.37	2.35	3.74	18.62				2.10
R = CH_2CH_3												
(DO)(DOH)pn	PF_6	7.43	7.17	7.15	2.35	2.32	3.85	19.14	4.04	3.67	2.40	2.31
(DO)(DOH)pn	ClO_4	7.65	7.19	7.14	2.35	2.32	3.91	19.12	4.13	3.68	2.42	2.31
$(DH)_2$		7.94	7.95	7.08	2.36	2.35	3.75	18.50				2.10
R = *neo*-C_5H_{11}												
(DO)(DOH)pn	ClO_4	7.47	7.13	7.06	2.34	2.31	3.87	19.40	4.19	3.66	2.45	2.30
$(DH)_2$		7.98	7.92	7.05	2.36	2.34	3.73	18.60				
R = *i*-C_3H_7[c]												
(DO)(DOH)pn	PF_6	7.31	7.12	7.10	*d*	*d*	3.81	18.94	4.02	3.69	2.40	2.31
$(DH)_2$		7.93	7.98	7.06	2.35	2.34	3.73	18.42				2.09
R = *c*-C_6H_{11}[c]												
(DO)(DOH)pn	ClO_4	7.55	7.18	7.11	2.33	2.31	3.89	18.95	4.12	3.69	2.42	2.31
$(DH)_2$		7.96	7.90	7.05	2.35	2.33	3.73					2.10

[a] Data from ref 6 and 42. [b] Signals consist of two multiplets; values given are the center of the multiplet. The downfield multiplet arises from the protons nearest L. The N—C—CH_2—C—N signals are obscured by the O—N=C—CH_3 signals in most cases and are not reported. [c] Exhibits broad L signals. [d] Obscured.

Table X. Chemical Shifts of ^1H NMR Signals of Me_3Bzm, $[Me_3BzmCo((DO)(DOH)pn)R]ClO_4$,[a] and $Me_3BzmCo(DH)_2R$[b] Complexes in DMSO-d_6

	chem shift								
compd	H2	H4	H7	$B10H_3$	$B11H_3$	$B12H_3$	O—H···O	C—N=C—CH_3	O—N=C—CH_3
Me_3Bzm	8.00	7.40	7.31	2.30	2.34	3.77			
R = CH_2CN									
(DO)(DOH)pn	7.65	7.41	7.12	2.28	2.30	3.82	19.04	2.51	2.34
$(DH)_2$	7.90	7.80	7.33	2.28	2.29	3.81	18.70		2.13
R = CH_2CF_3									
(DO)(DOH)pn	7.54	7.41	6.97	2.29	2.31	3.83	19.06	2.51	2.33
$(DH)_2$	7.90	7.83	7.32	2.27	2.29	3.80	18.68		2.09
R = CH_2Br									
(DO)(DOH)pn	7.68	7.42	7.09	2.27	2.30	3.83	18.98	2.47	2.30
$(DH)_2$	7.95	7.94	7.09	2.35	2.37	3.75			2.15
R = CH_3									
(DO)(DOH)pn	7.57	7.41	6.97	2.26	2.31	3.82	19.25	2.41	2.27
$(DH)_2$	7.87	7.79	7.33	2.27	2.30	3.80	18.84		2.04
R = CH_2CH_3									
(DO)(DOH)pn	7.53	7.40	6.92	2.27	2.29	3.81	19.15	2.43	2.28
$(DH)_2$	7.86	7.78	7.31	2.26	2.29	3.79	18.74		2.04
R = *neo*-C_5H_{11}									
(DO)(DOH)pn	7.38	7.35	6.82	*c*	*c*	*c*	19.46	*c*	*c*
$(DH)_2$	7.84	7.81	7.29	2.26	2.28	3.77	18.80		2.02

[a] The signals from the propylene protons are obscured by the same signals from the aqua adduct, the O—N=C—CH_3 signals, or the B12H$_3$ signals. [b] Data from ref 6 and 42. [c] Signals are broad and obscured.

The ^1H NMR spectrum of the *neo*-C_5H_{11} derivative in DMSO-d_6 has broad signals for free and coordinated Me_3Bzm. Spectra of $[Me_3BzmCo((DO)(DOH)pn)R]ClO_4$ (R = *i*-C_3H_7, c-C_6H_{11}) contain primarily signals for the DMSO adduct and free Me_3Bzm.

The ^1H NMR shifts for $[H_2OCo((DO)(DOH)pn)R]ClO_4$ in DMSO-d_6 (Table XI) do not correlate with EP. In this solvent, H_2O is probably replaced by DMSO-d_6. The equatorial methyl signals of the $CH_2C_6H_5$ derivative are the most upfield of the series. The upfield multiplet from N-CH_2-C-CH_2-N has an extreme upfield shift, assigning it to the H of each CH_2 closest to $CH_2C_6H_5$. The (DO)(DOH)pn ^1H NMR signals of the aqua derivatives (Table XI) change very little on Me_3Bzm coordination (Table X). The O–H···O signal is affected the most (ca. 0.1 ppm).

^{13}C NMR Studies. ^{13}C NMR data collected for nine [pyCo((DO)(DOH)pn)R]ClO_4 compounds[15] are given in Table XII. Only the $CH_2CO_2CH_3$, CH_3, and C_2H_5 derivatives were soluble to 0.1 M in $CDCl_3$. The others formed saturated solutions (10–70

Table XI. Chemical Shifts (ppm) of ^{1}H NMR Signals for $[H_2OCo((DO)(DOH)pn)R]ClO_4$ Complexes in DMSO-d_6

		chem shift						
R	EP[a]	O—H···O	N—CH_2—C—CH_2—N[b]		C—N=C—CH_3	O—N=C—CH_3	N—C—CH_2—C—N[b]	
CH_2CN	−0.75	18.89	3.93	3.75	2.53	2.39	2.07	1.95
CH_2CF_3	−0.55	18.97	4.00	3.63	2.49	2.35	2.17	1.84
$CH_2CO_2CH_3$	−0.49	18.92	3.94	3.60	2.49	2.35	2.21	1.83
CH_2Br	−0.44	18.83	3.84	3.67	2.46	2.33	2.10	1.93
CH_3	0	19.10	3.80	3.65	2.40	2.27	1.96	
$CH_2Si(CH_3)_3$	+0.06	19.22	3.90	3.63	2.43	2.29	2.12	1.82
$CH_2C_6H_5$	+0.08	19.08	3.90	3.47	2.26	2.16	*c*	1.78
CH_2CH_3	+0.12	19.05	3.84	3.55	2.40	2.27	2.02	1.85
neo-C_5H_{11}	+0.19	19.35	3.95	3.56	2.41	2.28	2.13	1.75
i-C_3H_7	+0.24	18.96	3.86	3.57	2.42	2.29	2.06	1.80
c-C_6H_{11}	+0.32	18.94	3.83	3.57	2.41	2.28	2.16	2.06

[a] Electronic parameter; see text. [b] Signals consist of two multiplets; values are the centers. [c] Obscured signal.

Table XII. Chemical Shifts (ppm) of ^{13}C NMR Signals of Pyridine and of $[pyCo((DO)(DOH)pn)R]ClO_4$ and $pyCo(DH)_2R$ Complexes in $CDCl_3$[a]

	chem shift								
compd	α	β	γ	C—N=*C*	O—N=*C*	N*C*$H_2$$CH_2$-*C*$H_2$N	NCH_2*C*H_2-CH_2N	C—N=C—*C*H_3	O—N=C—*C*H_3
py	149.92	123.73	135.89						
R = CH_2CF_3									
(DO)(DOH)pn	148.83	127.15	139.32	*b*	*b*	49.17	27.12	18.06	13.23
$(DH)_2$	149.94	125.42	138.03		150.84				12.22
R = $CH_2CO_2CH_3$									
(DO)(DOH)pn	148.85	127.09	139.17	176.07	155.51	49.04	27.06	18.20	13.35
$(DH)_2$	150.23	125.39	137.97		150.79				12.38
R = CH_2Br									
(DO)(DOH)pn	149.76	127.03	139.20	175.06	154.87	49.25	27.14	18.16	13.17
$(DH)_2$	150.34	125.37	137.96		150.34				12.31
R = CH_3									
(DO)(DOH)pn	148.77	126.76	138.73	173.56	153.71	49.50	27.30	17.64	12.92
$(DH)_2$	150.06	125.21	137.48		148.98				11.98
R = $CH_2Si(CH_3)_3$									
(DO)(DOH)pn	148.42	126.81	138.70	173.81	154.44	49.43	27.21	17.75	13.09
$(DH)_2$	149.68	125.14	137.42		149.59				12.10
R = $CH_2C_6H_5$									
(DO)(DOH)pn	148.95	126.80	138.65	174.04	153.95	48.93	27.19	17.54	12.94
$(DH)_2$	150.32	125.15	137.36		149.29				
R = CH_2CH_3									
(DO)(DOH)pn	148.74	126.72	138.55	173.49	153.75	49.24	27.13	17.61	12.91
$(DH)_2$	150.10	125.16	137.34		149.01				11.95
R = *neo*-C_5H_{11}									
(DO)(DOH)pn	148.00	126.71	138.51	173.99	*b*	48.71	27.09	17.66	13.01
$(DH)_2$	149.54	125.05	137.29		149.94				12.04
R = *i*-C_3H_7									
(DO)(DOH)pn	148.56	126.66	138.47	*b*	*b*	48.92	27.05	17.70	12.93
$(DH)_2$	150.01	125.04	137.21		149.30				12.00

[a] Data for $(DH)_2$ complexes from ref 6 and 42. [b] Data not collected.

mM). The c-C_6H_{11} derivative was too insoluble to study.

The ^{13}C signals of the two types of N=C and methyl carbons of the (DO)(DOH)pn moiety were assigned by analogy to the $(DH)_2$ complexes (Table XII). These N=C and methyl signals move upfield, in general, as the electron-donating ability of the alkyl group increases.

The ^{13}C signals for the py β-C and γ-C atoms shift downfield on coordination (Table XII) and are ca. 1.0 and 1.7 ppm further downfield, respectively, in the (DO)(DOH)pn complexes relative to the analogous $(DH)_2$ complexes. These resonances follow the trans influence of R in the same way for the (DO)(DOH)pn and $(DH)_2$ complexes as evidenced from the linear relationship, with slope = 0.995 (lcc = 0.9946 for nine points), between the ^{13}C NMR γ-C of py shifts (supplementary).

The py β-C and γ-C ^{13}C NMR signals shift upfield with increasing EP value (1.6 and 0.9 ppm for the (DO)(DOH)pn series and 0.4 and 0.9 ppm for the $(DH)_2$ series, respectively; Table XII). Upon coordination to Co((DO)(DOH)pn)R, the py α-C ^{13}C signal is shifted upfield (0.9 ppm average, Table IX). Coordination of py to $Co(DH)_2R$ shifted the α-C ^{13}C signal downfield (0.2 ppm average), except for the $CH_2Si(CH_3)_3$ and *neo*-C_5H_{11} derivatives, in which the α-C ^{13}C signal shifted upfield (0.24 and 0.38 ppm, respectively). The CH_2Br derivatives in both systems have extreme downfield py α-C ^{13}C py shifts (Table XII). No correlation exists between EP and the py α-C ^{13}C signals for either model system.

The ^{13}C signals for the $[Me_3BzmCo((DO)(DOH)pn)R]ClO_4$ complexes in $CDCl_3$ (Table XIII), assigned by comparison to previous data,[34,35,38] are well-resolved sharp lines except for those for the *neo*-C_5H_{11} derivative. It exhibited broad signals for the N=C carbons of (DO)(DOH)pn and for the Me_3Bzm carbons. The solubility of the methyl derivatives was limited (ca. 50 mM). As with the equatorial ^{13}C signals for the py derivatives, the C—N=*C* signal undergoes the greatest (3.2 ppm) and the NCH_2*C*$H_2$$CH_2$N signal undergoes the smallest (0.5 ppm) shift changes across the series.

Only the B5, B6, B8, and B12 signals correlate with EP (supplementary figures[45]). The best correlation with EP is for the B12 signal. As expected, derivatives with strong trans effect alkyl groups (e.g. CH_2CH_3) have Me_3Bzm ^{13}C shifts most similar to those of free Me_3Bzm.

In $CDCl_3$, most of the ^{13}C signals of Me_3Bzm (i.e. B2, B5, B6, B7, B10, B11, and B12) shift downfield upon coordination in the

Table XIII. Chemical Shifts (ppm) of ^{13}C NMR Signals for Me_3Bzm and for $[Me_3BzmCo((DO)(DOH)pn)R]ClO_4$ and $Me_3BzmCo(DH)_2R$[a] Complexes in $CDCl_3$

compd	B2	B4	B5	B6	B7	B8	B9	B10	B11	B12	C—N=*C*	O—N=*C*	N*C*H₂CH₂-*C*H₂N	NCH₂*C*H₂-CH₂N	C—N=C—*C*H₃	O—N=C—*C*H₃
Me_3Bzm	142.80	120.29	132.05	130.84	109.51	133.21	142.50	20.53	20.20	30.87						
R = CH_2CN																
(DO)(DOH)pn	144.34	116.81	134.01	133.18	111.12	133.34	139.39	20.72	20.27	32.16	175.84	155.73	49.21	27.68	18.62	13.40
$(DH)_2$	143.44	118.62	133.68	133.19	109.92	132.75	140.05	20.56	20.40	31.89		150.98				12.61
R = CH_2CF_3																
(DO)(DOH)pn	144.18	116.58	133.68	132.80	111.19	133.57	139.18	20.78	20.23	32.11	175.75	155.46	49.25	27.23	17.92	13.14
$(DH)_2$	143.45	118.73	133.50	132.99	109.84	132.78	139.93	20.53	20.33	31.82		150.75				12.18
R = $CH_2CO_2CH_3$																
(DO)(DOH)pn	144.41	116.63	133.60	132.69	111.20	133.60	139.39	20.81	20.22	32.10	175.34	155.26	49.05	27.16	18.00	13.25
$(DH)_2$	143.54	118.89	133.41	132.92	109.74	132.84	140.12	20.50	20.38	31.80		150.56				12.33
R = CH_2Br																
(DO)(DOH)pn	144.62	117.06	133.67	132.84	110.98	133.44	139.71	20.72	20.27	32.04	174.48	154.79	49.25	27.23	18.00	13.13
$(DH)_2$	143.17	118.88	133.41	132.92	109.79	132.79	140.31	20.55	20.43	31.79		150.17				12.31
R = CH_3																
(DO)(DOH)pn	144.34	117.14	133.35	132.42	110.81	133.56	140.02	20.68	20.28	31.89	172.62	153.32	49.39	27.43	17.43	12.87
$(DH)_2$	143.64	119.17	133.09	132.96	109.66	132.57	140.72	20.50	20.40	31.66		148.84				11.97
R = CH_2CH_3																
(DO)(DOH)pn	144.31	117.16	133.23	132.29	110.82	133.64	140.08	20.69	20.25	31.85	172.73	153.43	49.15	27.18	17.43	12.87
$(DH)_2$	143.74	119.24	133.01	133.01	109.64	132.46	140.81	20.47	20.47	31.63		148.95				11.96
R = *neo*-C_5H_{11}																
(DO)(DOH)pn	144.15	116.94	133.10	132.08	110.97	133.77	139.74	20.62	20.21	31.87	173.63	155.12	48.70	27.26	17.51	13.01
$(DH)_2$	143.47	119.21	132.96	132.85	109.54	132.55	140.44	20.43	20.43	31.62		149.79				12.02

[a] Data from ref 6 and 42.

Table XIV. Chemical Shifts (ppm) of ^{13}C NMR Signals for Me_3Bzm and for $[Me_3BzmCo((DO)(DOH)pn)R]ClO_4$ and $Me_3BzmCo(DH)_2R$[a] Complexes in DMSO-d_6

compd	B2	B4	B5	B6	B7	B8	B9	B10	B11	B12	C—N=*C*	O—N=*C*	N*C*H₂CH₂-*C*H₂N	NCH₂*C*H₂-CH₂N	C—N=C—*C*H₃	O—N=C—*C*H₃
Me_3Bzm	143.56	119.31	130.71	129.52	110.03	133.12	141.98	19.96	19.79	30.45						
R = CH_2CN																
(DO)(DOH)pn	144.56	116.13	132.90	132.13	111.52	132.90	138.67	20.28	19.63	31.71	175.84	156.05	48.62	26.94	18.14	13.13
$(DH)_2$	143.78	117.28	132.60	131.67	110.96	132.60	139.07	20.17	19.71	31.56		150.78				12.20
R = CH_2CF_3																
(DO)(DOH)pn	144.11	116.01	132.75	132.02	111.55	133.05	138.48	20.26	19.61	31.68	175.82	156.08	48.52	26.70	17.57	12.90
$(DH)_2$	143.64	117.36	132.46	131.54	110.87	132.58	138.96	20.13	19.70	31.51		150.57				11.82
R = $CH_2CO_2CH_3$[b]																
(DO)(DOH)pn	144.24	116.04	132.71	132.00	111.54	133.10	138.71	19.92	19.75	31.64	175.44	155.61	48.42	26.53	17.61	12.93
R = CH_2Br																
(DO)(DOH)pn	144.67	116.41	132.75	131.97	111.42	132.96	139.01	20.28	19.69	31.62	174.92	155.28	48.61	26.66	17.65	12.86
$(DH)_2$	143.85	117.49	132.38	131.46	110.82	132.62	139.34	20.14	19.85	31.44		149.91				11.90
R = CH_3																
(DO)(DOH)pn	144.23	116.39	132.48	131.69	111.32	133.12	139.39	20.28	19.69	31.47	173.11	153.86	48.79	26.87	17.12	12.54
$(DH)_2$	143.75	117.88	132.14	131.17	110.69	132.75	139.73	20.12	19.79	31.34		148.47				11.60
R = CH_2CH_3																
(DO)(DOH)pn	144.19	116.47	132.48	131.54	111.29	133.09	139.40	20.24	19.67	31.46	173.05	153.84	48.50	26.72	17.09	12.54
$(DH)_2$	143.79	117.94	132.08	131.09	110.62	132.79	139.83	20.12	19.77	31.32		148.53				11.56

[a] References 6 and 42. [b] The $(DH)_2$ derivative has very poor solubility in DMSO-d_6.

Table XV. Comparison of Relevant Geometric Parameters for LCo(chel)R Complexes[a]

R	Co–C, Å	Co–N, Å	N–Co–C, deg	α, deg	d, Å
L = Me_3Bzm					
chel = (DO)(DOH)pn					
CH_2CF_3	2.026 (4)	2.060 (3)	173.9 (1)	16.6	0.06
CH_3	2.011 (3)	2.100 (3)	177.4 (1)	13.8	0.09
CH_2CH_3	2.041 (4)	2.105 (3)	175.5 (2)	16.7	0.10
chel = $(DH)_2$[b]					
$CHCl_2$	1.983 (2)	2.043 (2)	173.72 (8)	1.5	0.01
CH_3	1.989 (2)	2.060 (2)	176.8 (1)	4.7	0.06
i-C_3H_7	2.076 (2)	2.097 (2)	176.41 (8)	4.0	0.01
L = py					
chel = (DO)(DOH)pn[c]					
CH_3	2.003 (3)	2.106 (3)	178.9 (1)	6.9	0.07
neo-C_5H_{11}	2.083 (4)	2.121 (3)	177.1 (2)	14.3	0.03
chel = $(DH)_2$[d]					
CH_2CF_3[e]	2.010 (3)	2.041 (2)	174.6 (1)	1.0	0.01
CH_3	1.998 (5)	2.068 (3)	178.0 (2)	3.2	0.04
CH_2CH_3[f]	2.035 (5)	2.081 (3)	177.1 (2)	9.1[g]	0.05
neo-C_5H_{11}	2.060 (6)	2.081 (4)	174.7 (2)	−5.2	0
i-C_3H_7	2.085 (3)	2.099 (2)	174.1 (2)	4.0	0.02
chel = cobalamin[h]					
CH_3	1.99 (2)	2.19 (2)	171 (1)		
5′-deoxyadenosyl	2.03 (3)	2.24 (3)	170 (2)		

[a] Positive values of α and *d* indicate bending of the equatorial ligand toward the alkyl group and displacement of Co out of the plane of N4 equatorial donors toward L. [b] Reference 42. [c] Reference 15. [d] Reference 6. [e] The neutral ligand is 4-CNpy. [f] The neutral ligand is 4-HN=C(OCH_3)py. [g] Twisted. [h] References 9 and 10.

(DO)(DOH) pn or $(DH)_2$, derivatives. On coordination, the B8 signal shifts downfield in all (DO)(DOH) pn complexes and upfield in all $(DH)_2$ complexes (Table XIII). The change in shift on coordination to Co(DO)(DOH)pn or $Co(DH)_2$ is greatest for B4 and B9 (upfield). Thus, as found for py, L nuclei close to Co in the (DO)(DOH)pn derivatives are shielded (relative to free L) much more than in the (DH_2) complexes. All other L nuclei in (DO)(DOH)pn derivatives have signals downfield from those of the corresponding $(DH)_2$ derivatives.

The six equatorial (DO)(DOH)pn ^{13}C signals of the aqua derivatives in DMSO-d_6 are given in the supplementary material.[45] The signals of the N=C and methyl carbons in the DMSO adducts shift upfield with increasing EP of R. Coordination of Me_3Bzm causes downfield shifts of all these signals except for the O—N=*C* and the $NCH_2CH_2CH_2N$ signals, which shift upfield (Table XIV). Because of ligand exchange, data for some derivatives are not reported. Assignments are based on those for α-ribazole in DMSO-d_6[35] and coenzyme B_{12} in D_2O.[38] The B5, B6, B8, and B12 signals have good to very good correlations with EP (supplementary material[45]), whereas the B7 and B9 signals give poor correlations. B2 and B4 show no trends. Except for the B4, B8, B9, and B11 signals, the Me_3Bzm ^{13}C signals shift downfield upon coordination to Co((DO)(DOH)pn)R (Table XIV).

Discussion

Structures. This paper reports the first structures of Costa's B_{12} model containing a benzimidazole ligand (Me_3Bzm). The geometry of the axial fragment is compared with that in cobaloximes and cobalamins in Tables XV and XVI, which also contain data for analogous py complexes. As already observed,[6] the Co–C bond length is scarcely influenced by changing the equatorial or L ligands, but it depends mainly on the bulk of the R ligand.

In contrast, the Co–N(axial) distances, which increase with increasing R σ-donor power, are also significantly influenced by the nature of the equatorial ligand.[6] Thus, for both Me_3Bzm and py complexes, this bond is longer in (DO)(DOH)pn than in $(DH)_2$ compounds with the same R. This lengthening is accompanied by large α and *d* values, particularly for Me_3Bzm complexes.

Table XVI. Comparison of Geometrical Parameters of the Co–CH_2CH_3 Group and the α Angles in LCo(chel)CH_2CH_3 Complexes

chel	L	C–C, Å	Co—CH_2—CH_3, deg	α, deg
(DO)(DOH)pn	Me_3Bzm[a]	1.380 (8)	124.5 (4)	16.7
	$PhNH_2$[b]	1.480 (7)	118.7 (3)	−7.1
	H_2O[c]	1.496 (5)	117.7 (3)	−9.3
$(DH)_2$	PPh_3[d]	1.317 (9)	126.2 (5)	1.4
	2-NH_2py[g]	1.434 (6)	121.0 (3)	4.0
	4-NH=C(OCH_3)py[d]	1.519 (8)	117.8 (4)	9.1[e]
	$PhNH_2$[f]	1.479 (6)	117.8 (3)	2.8

[a] Present work. [b] Unpublished results. [c] To be submitted for publication. [d] Reference 6. [e] Twisted. [f] Reference 43. [g] Marzilli, L. G.; Summers, M. F.; Zangrando, E.; Bresciani-Pahor, N.; Randaccio, L. *J. Am. Chem. Soc.* **1986**, *108*, 4830.

In (DO)(DOH)pn complexes with L = py[15] or Me_3Bzm, orientations close to A (Figure 4a) are observed. For analogous cobaloximes, orientation B is observed.[6,42] Recent studies on cobaloximes show that imidazole ligands may have either orientation.[41] However, orientation B is favored by the shorter Co–N(axial) bond. Therefore, for the same R, the larger values of Co–N distances, α and *d* in (DO)(DOH)pn than in $(DH)_2$ complexes probably can be attributed mainly to the different orientation of the planar L ligand. In orientation A, the planar L should interact with (DO)(DOH)pn more strongly than in orientation B. On the contrary, comparison of $(DH)_2$ and (DO)(DOH)pn complexes with nonplanar, i.e. "nondirectional" ligands, such as PPh_3 or $P(OCH_3)_3$, shows[16] no significant difference in the Co–P bond lengths for the two series. These results clearly show that substitution of a –O···HO– by –CH_2–CH_2–CH_2– in the equatorial ligand causes an increase in the Co–N axial distance, accompanied by an increase in α and *d* values, for complexes with planar L. Therefore, in cobalamins, in which the corrin ring has a large number of side groups, interaction of the latter with the benzimidazole moiety may influence the axial Co–N bond length. Consequently, although less accurate values are compared for cobalamins, it is not surprising to find the following order of increasing Co–N bond length: $(DH)_2$ < (DO)(DOH)pn < Schiff base < corrin. This observation would also suggest that, in coenzyme B_{12}, induced changes in the orientation of the benzimidazole moiety may provoke significant changes in the Co–N axial bond length. It is noteworthy that, for the same equatorial ligand, the Co–N distance, α and *d* values in Me_3Bzm and py analogues do not differ significantly. Comparison with imidazole derivatives[41] suggests the following order of increasing Co–N bond length in both cobaloximes and Costa's models: imidazole < py ~ Me_3Bzm. This trend may be interpreted by assuming that the C–N–C angle of ~105° in the imidazole ligands, significantly narrower than the ~120° angle in py ligands, allows a shorter Co–N distance in the former. The C–N–C angle in Me_3Bzm is still ~105°. The increased bulk, due to the fused six-membered ring, distorts the coordination around nitrogen (see above) and lengthens the Co–N bond. The net result is that the Co–N distances are similar in py and Me_3Bzm analogues.

The structures of I–III reveal a large bending of the symmetrical halves of the (DO)(DOH)pn moiety toward R. The α angles (13.8–16.7°) can be compared to the 14.3° angle found in [pyCo((DO)(DOH)pn)-*neo*-C_5H_{11}]PF_6.[15] The largest α angles have been found in complexes containing bulky planar L ligands. [1,2-Me_2ImdCo((DO)(DOH)pn)CH_3]$^+$ has the largest α (19.7°) of any Costa-type complex studied to date.[15–19,42] Although the folding of the (DO)(DOH)pn moiety is away from Me_3Bzm, the propylene bridge is puckered toward Me_3Bzm (Figures 1–3). The pucker of this six-membered ring is usually away from the bulkier axial ligand, e.g. toward R in [pyCo((DO)(DOH)pn)CH_3]PF_6 and toward L in [pyCo((DO)(DOH)pn)-*neo*-C_5H_{11}]PF_6.[15] Steric interaction of R with the equatorial moiety provokes (a) the opening of the Co–CH_2–X angle up to 124.5 (4)° in II and 124.4

(41) Bresciani-Pahor, N.; Marzilli, L. G.; Randaccio, L.; Toscano, P. J.; Zangrando, E., *J. Chem. Soc., Chem. Commun.* **1984**, 1508.
(42) Unpublished results.

(3)° in III and (b) a shortening of the C–CH_3 bond (1.380 (8) Å) in II and of the C–CF_3 bond (1.436 (6) Å) in III. A widening of the Co–CH_2–CH_3 angle and a corresponding shortening of the CH_2–CH_3 (also observed in ethylcobaloximes) appear to be related to the bulk of L and to the bending of the equatorial moiety (Table XVI). For example, the C–C bond length increases whereas the Co–C–C bond angle decreases with decreasing bulk of L.

Rates. In noncoordinating solvents, L exchange in these complexes follows a first-order rate law consistent with an S_N1 LIM mechanism.[6,15-19] Reactivities of Costa-type complexes average 10 times greater than those of the analogous cobaloxime complexes.[16] Here we have found the same relationship for Me_3Bzm adducts.

Correspondingly, the Co–N (axial) distances for py and Me_3Bzm complexes having the same L–Co–R fragment are about 0.04 Å shorter in cobaloximes (Table XV). On the contrary, when corresponding $(DH)_2$ and (DO)(DOH)pn complexes are compared for L = aniline ($PhNH_2$), the difference in the Co–NH_2Ph distances is smaller. In CH_3 and CH_2CH_3 compounds, the Co–NH_2Ph distance is only 0.025 Å longer in Costa's model, while the rate constants are 0.50 s^{-1} for $[PhNH_2Co((DO)(DOH)pn)CH_3]^+$ and 1.51 s^{-1} for $PhNH_2Co(DH)_2CH_3$.[17,42,43] On the other hand, the orientation of aniline with respect to the equatorial ligand in cobaloximes is very similar to that in the (DO)(DOH)pn compounds. Analogous behavior was found for these two LCo(chel)CH_3 series with L = $P(OCH_3)_3$ and PPh_3.[16]

The dissociation rate of L from $[(py)Co((DO)(DOH)pn)CH_3]ClO_4$ ($k_1 = (3.6 \pm 0.1) \times 10^{-2}$ s^{-1})[15] in CH_2Cl_2 (25 °C) is slightly slower than the rate from $[Me_3BzmCo((DO)(DOH)pn)CH_3]ClO_4$. In DMSO, the Me_3Bzm adduct has a slightly higher formation constant (75 M^{-1}) than the py adduct (56 M^{-1}). Thus, the py and Me_3Bzm ligands have a very similar affinity for this Costa derivative. The Costa compounds also form weak Me_3Bzm adducts with derivatives containing strongly electron-donating alkyl groups (i-C_3H_7, c-C_6H_{11}), especially in DMSO. However, with $Me_3BzmCo(DH)_2R$ in DMSO-d_6, only a trace amount of the DMSO adduct is detected by ^1H NMR spectroscopy.

^{1}H NMR Spectroscopy. The ^1H NMR spectra of some Costa-type organocobalt complexes have been relatively little studied[16,17,20,21,26,28-30,44] compared to those for the cobaloxime complexes.[6] This lack of information is due in part to the greater difficulty in preparing the former complexes.

^1H NMR shifts are known to be sensitive to anisotropic effects.[6] Indeed, the H's nearest to the $Co((DO)(DOH)pn)R^+$ moiety in py (α-H) and Me_3Bzm (H2, H4) are shielded in the adducts relative to free base (Tables VIII–X). In DMSO-d_6 the H4 signal is essentially unaffected by coordination to $Co((DO)(DOH)pn)R^+$ (Table X).

On coordination to $Co(DH)_2R$ the α-H shift of py is affected very little. The H2 and H4 signals of Me_3Bzm both shift downfield in $CDCl_3$ on coordination to $Co(DH)_2R$ (Table IX). In DMSO-d_6 the H4 signal also moves downfield, but the H2 signal moves slightly upfield (Table X).

The downfield shifting of H2 and H4 Me_3Bzm signals on coordination to cobaloximes and upfield shifting of these signals on coordination to Costa-type complexes are not affected by the nature of R. We are unable to determine conclusively if the greater anisotropy in the Costa complexes results from the Co or from the Co–N–C–C–N chelate rings. But, from crystal structures of $Me_3BzmCo(DH)_2R$, H2 and H4 are over the Co–N–O···H–O–N rings.[42] The ^1H NMR shifts are also consistent with H2 and H4 being outside the shielding effects of an anisotropic ring system. Thus, it seems that the greater anisotropic effect on L in the (DO)(DOH)pn system compared to the $(DH)_2$ system could result from different L orientations.

^{13}C NMR Spectroscopy. The ^{13}C NMR data in Tables XII–XIV and the supplementary material[45] provide a basis for comparison of shift trends in Costa-type complexes with cobaloximes. Some data are also available for the alkylcobalamins.[34,38] The shifts of B5, B6, B7, B9, and B12 are similarly influenced by R in both model systems. Signals for B2 and B4 shift erratically in both series. The B8 signal is affected quite differently in the two model systems although it follows EP in the Costa-type compounds (supplementary figures[45]).

The ^{13}C signals from L nuclei remote from the anisotropic equatorial unit are linear with EP, correlate well between the two model systems, and are a good measure of the trans influence of R. The ^{13}C shifts of the γ-C of 4-*tert*-butylpyridine in the $(DH)_2$ complexes are known to have an excellent correlation with the Co–N(py) bond lengths of the corresponding py complexes.[6] The γ-C of py and B12 of Me_3Bzm have signals that correlate very well with each other and between the two model systems. These signals are downfield in the Costa-type complexes, relative to the cobaloximes, suggesting that the former are relatively electron deficient.

The ^{13}C shifts of remote L nuclei approach the shifts of the free ligand for complexes with the strongest electron-donor R. The ^{13}C signals of L nuclei remote from Co are deshielded compared to L. Signals of B4 and B9 of Me_3Bzm and α-C of py nuclei close to the equatorial moiety are shielded on coordination. The B2 signal of coordinated Me_3Bzm, although close to Co, is downfield from B2 of free Me_3Bzm in both model systems. This indicates that B2 is more sensitive to through-bond effects than B4 and B9.

Aside from the magnitude of the ^{13}C shift changes (which are in general greater in Costa-type complexes than to cobaloximes), the two equatorial units shift the signals of Me_3Bzm nuclei in similar directions (Tables XIII and XIV). These shift trends are also observed for N3 protonation of α-ribazole[34] and for dimethylbenzimidazole in the coenzyme in D_2O,[11] except that B2 is shifted upfield, relative to free base.

Conclusions

All of our observations on L dissociation rates, structure, and NMR spectra of Costa vs cobaloxime models can be understood from a combination of electronic effects (greater electrophilicity of the Co center in Costa models) and steric effects (the puckered propylene bridge).

The compounds structurally characterized here exhibit the typical trend, III < I < II, in Co–N(axial) bond length, and the ^{13}C shifts of remote L carbons follow this trend. The relationship between such shifts in cobaloximes and Costa models further argues that the dependence of such shifts on Co–N(axial) bond length will be a general phenomenon. NMR methods thus continue to hold promise as a means of gaining insight into cobalamin conformational changes.

Acknowledgment. This research was supported by NIH Grant GM 29225 to L.G.M. and by a grant from the MPI (Rome) to L.R. The purchase of the 360-MHz NMR instrument was supported in part by an NSF departmental grant to Emory. We are grateful to these organizations.

Supplementary Material Available: Figures showing selected ^{13}C shifts plotted vs EP and plots of log k_1 for the (DO)(DOH)pn system vs log k_1 for the $(DH)_2$ systems and the ^{13}C NMR shifts for the γ-C of py for the (DO)(DOH)pn vs the $(DH)_2$ systems and tables of elemental analyses, ^{13}C NMR shifts of $[H_2OCo((DO)(DOH)pn)R]ClO_4$ in DMSO-d_6, anisotropic thermal parameters, hydrogen atom coordinates, and complete bond lengths and bond angles (23 pages); tables of structure factors (50 pages). Ordering information is given on any current masthead page.

(43) Marzilli, L. G.; Bayo, F.; Summers, M. F.; Thomas, L. B.; Zangrando, E.; Bresciani-Pahor, N.; Mari, M.; Randaccio, L. *J. Am. Chem. Soc.* **1987**, *109*, 6045.
(44) Dimmit, J. F.; Weber, J. H. *Inorg. Chem.* **1982**, *21*, 700.
(45) See paragraph at end of paper regarding supplementary material.